Proceedings of Ninth World Conference on Earthquake Engineering
August 2-9, 1988, Tokyo-Kyoto, JAPAN (Vol.III)

5-1-4

SOIL-STRUCTURE INTERACTION ANALYSIS BY USING CLONING ALGORITHM

Ken'ichi MORIYAMA[1], Gautam DASGUPTA[2], and Masanobu SHINOZUKA[3]

[1]Taisei Corporation, Tokyo, JAPAN
[2]Department of Civil Engineering and Engineering Mechanics, Columbia University, New York, New York, USA
[3]Department of Civil Engineering and Operations Research, Princeton University, Princeton, New Jersey, USA

SUMMARY

A method to perform the soil-structure interaction analysis is presented. The system is divided into two subsystems. The first is the near-field which includes superstructures, embedded foundations and irregular soil regions and the other is the elastic unbounded region (far-field). The near-field is modeled by Finite Element Method to represent local irregularities. The far-field is represented in the form of boundary (frequency dependent) impedance matrix according to a cloning algorithm. The efficiency of the cloning algorithm is demonstrated and various types of soil-structure interaction systems are analyzed to capture their dynamic response characteristics.

INTRODUCTION

It is well-known that the phenomenon of soil-structure interaction greatly affects the dynamic response of structures, especially one which is larger or long in size, such as a nuclear power plant or a long-span bridge. However, it is not a routined procedure to calculate such responses because a soil-structure interaction system consists of two quite different subsystems from the mechanics point of view. The system is divided into the near- and far-fields. Because of its flexibility in modeling and capability of nonlinear analysis, the Finite Element Method is used to represent the near-field. The far-field is an elastic unbounded region which satisfies Sommerfeld's radiation condition. Its effect is represented as a boundary impedance matrix by using the cloning algorithm. The cloning algorithm needs no analytical formulation and uses only the conventional finite element formulation involving matrix inversion and eigenvalue-related calculation, which can be easily accomplished using standard available mathematical library packages. Also, the cloning method has been tested to be quite versatile.

FORMULATION OF THE GOVERNING EQUATIONS

Equation of Motion A soil-structure interaction system is divided into two subsystems, the near- and far- fields, as shown in Fig. 1 (Ref. 2,6). To take the advantage of versatility in modeling, the near-field is represented with finite elements. The far-field is represented as the boundary impedance which is calculated according to the cloning algorithm. Following the substructure method, the equation of motion of the soil-structure interaction system in the frequency domain is written as follows:

$$\left[-\omega^2 \begin{bmatrix} M_{ss} & M_{si} \\ M_{is} & M_{ii} \end{bmatrix} + \begin{bmatrix} K_{ss} & K_{si} \\ K_{is} & K_{ii}+K_i^* \end{bmatrix} \right] \begin{Bmatrix} u_s \\ u_i \end{Bmatrix} = \begin{Bmatrix} f_s \\ K_i^* \hat{u}_i \end{Bmatrix} \quad (1)$$

where

- i : degrees of freedom on boundary
- s : degrees of freedom other than i
- M_{jl} : mass submatrix with j, l degrees-of-freedom
- K_{jl} : stiffness submatrix with j, l degrees-of-freedom
- f_i : external force vector
- u_j : absolute displacement vector corresponding to j degrees-of-freedom
- K_i^* : boundary matrix of far-field
- $\hat{u}_i$: absolute displacement of soil with excavation (for ground excitation).

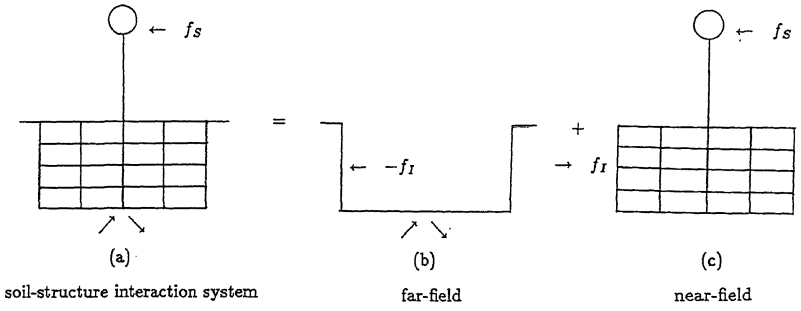

Fig. 1 Far-Field and Near-Field

Boundary Impedance Matrix of the Far-Field The boundary impedance of the far-field is obtained by using a cloning algorithm (Refs. 2,3) which concieves the unbounded region $B^{(\alpha)}$ as a summation of infinite number of geometrically similar cells $F^{(m)}$ as shown in Fig. 2. The boundary impedance $D^{(\alpha)}$ for the unbounded region $B^{(\alpha)}$ is computed from the dynamic stiffness matrix pertaining to $F^{(\alpha)}$. The force-displacement relationship can be written to be:

$$P^{(\alpha)} = D^{(\alpha)} u^{(\alpha)}, \quad \alpha = 1, 2 \quad (2)$$

where

- $P^{(\alpha)}$: force vector of $B^{(\alpha)}$
- $D^{(\alpha)}$: boundary impedance matrix of $B^{(\alpha)}$
- $u^{(\alpha)}$: displacement vector of $B^{(\alpha)}$

The equilibrium equation of cell $F^{(1)}$ is written in terms of the dynamic stiffness matrix of the cell element as follows:

$$\begin{Bmatrix} P_1 \\ P_2 \end{Bmatrix} = \begin{bmatrix} S_{11} & S_{12} \\ S_{21} & S_{22} \end{bmatrix} \begin{Bmatrix} u_1 \\ u_2 \end{Bmatrix} \quad (3)$$

where

- P_1, P_2 : force vector of cell element $F^{(1)}$
- u_1, u_2 : displacement vector of cell element $F^{(1)}$
- S_{ij} : stiffness submatrix of cell element $F^{(1)}$ with i, j degrees-of-freedom

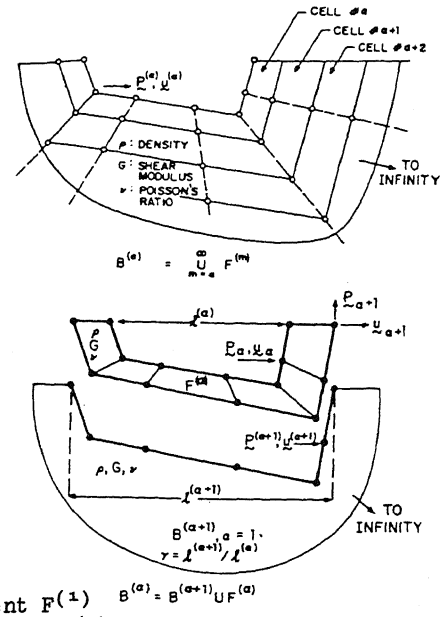

$B^{(\alpha)} = \sum_{m=\alpha}^{\infty} F^{(m)}$

$B^{(\alpha)} = B^{(\alpha+1)} U F^{(\alpha)}$

Fig. 2 Unbounded Region of Similar Geometry and a Finite Element Cell (Ref. 2)

Substituting Eq.(2) into Eq.(3) with compatibility conditions between $B^{(\alpha)}$ and $F^{(\alpha)}$, i.e., $u^{(\alpha)}=u_\alpha$, $\alpha=1,2$ and $P^{(1)}=P_1$, $P^{(2)}+P_2=0$, and eliminating u_α, $\alpha=1,2$, the following substructure equation can be obtained.

$$D^{(1)} = S_{11} - S_{12} \left[D^{(2)} + S_{22} \right]^{-1} S_{21} \tag{4}$$

The only difference between $D^{(1)}$ and $D^{(2)}$ is associated with the characteristic length $l^{(1)}$ and $l^{(2)}$. If $l^{(2)}$ is chosen close enough to $l^{(1)}$, $D^{(2)}$ can be approximated by $D^{(1)}$. Therefore, Eq.(4) can be solved for boundary impedance $D^{(1)}$.

NUMERICAL RESULTS AND DISCUSSIONS

Horizontal Impedance Function of Rigid Foundation on Elastic Half Space The horizontal impedance function of rigid foundation on an elastic half space was evaluated by using a model as shown in Fig. 3. A result from FLUSH (Ref. 5), which was calculated by using a viscous boundary at the bottom of the model and a result from the current method by using the same boundary as FLUSH at the bottom and the third direction and a boundary impedance matrix calculated from the cloning algorithm instead of the transmitting boundary, are compared in Fig. 4. Both results are almost the same.

Response Analysis The response acceleration of a rigid structure due to input ground motion of Fig. 5 was calculated. Two cases were examined. The first case involves the model shown in Fig. 6 and the ground motion was specified at the rigid base 120 meter below the free surface. The second case deals with the model shown in Fig. 7 where the ground motion was specified on the free surface. In each case the acceleration was calculated for three embedment conditions (H=0, 10, and 20 meter). The transfer function and the acceleration are shown in Fig. 8-11. The transfer function is defined as the ratio of the response displacement to the displacement at the control point. In all cases, the peak values of the transfer function and the maximum acceleration decrease as the embedment becomes deeper. The transfer functions for case 1 have more than one peak due to the surface layering effect.

Displacement Field Due to Ground Motion Displacement fields due to incident P- or SV-waves were calculated by using a soil model shown in Fig. 12 and the results were compared with that of the wave propagation theory. Horizontal displacements of the surface (z=0.0) due to vertical incident SV-waves were calculated for various impedance ratios $\alpha=(\rho_1 Cs_1)/(\rho_2 Cs_2)$ of Table 1 as shown in Fig. 13. The displacements agree well with the results of the wave propagation theory. The horizontal and vertical displacements of the surface due to P- and SV-waves with an incident angle were calculated as shown in Fig. 14-17. Here too the comparisons with the results of the wave propagation theory show good agreement.

CONCLUSIONS

Based on the results presented in this paper, the following conclusions can be drawn :

(1) Boundary impedance calculated by using the cloning algorithm satisfactorily represents the nature of radiation damping.

(2) Appropriate modeling method can be chosen by dividing the soil-structure interaction system into near- and far-fields. Good overall agreements with the theoretical results are anticipated.

ACKNOWLEDGMENT

This research was partially supported by the National Center for Earthquake Engineering Research under Contract Number 87-1313 and 87-1006 under master NSF Contract Number ECE-86-07591. The authors are also grateful to Taisei Corporation's support for this research.

REFERENCES

1. Bathe, K.-J., Finite Element Procedures in Engineering Analysis, Prentice Hall, Inc., (1982)
2. Dasgupta, G., "Finite Element Formulation for Unbounded Homogeneous Continua," Journal of Applied Mechanics, ASME, 49, 136-140, (1982)
3. Dasgupta, G.,"Sommerfeld's Radiation Condition and Cloning Algorithm," New Concepts in Finite Element Methods, Proceeding of ASME Summer Conference, Boulder, Colo., (1981)
4. Haskell, N. A., "The Dispersion of Surface Waves in Multilayered Media," Bulletine of the Seismological Society of America, 43, 17-34, (1953)
5. Lysmer, J., Udaka, T., Tsai, C.-F. and Seed, H.B., "FLUSH - A Computer Program for Approximate 3-D Analysis of Soil-Structure Interaction Problems," Earthquake Engineering Research Center Report UCB/EERC-75/30, University of California, Berkeley, (1975)
6. Wolf, J.P., Dynamic Soil-Structure Interaction, Prentice Hall, Inc. (1985)

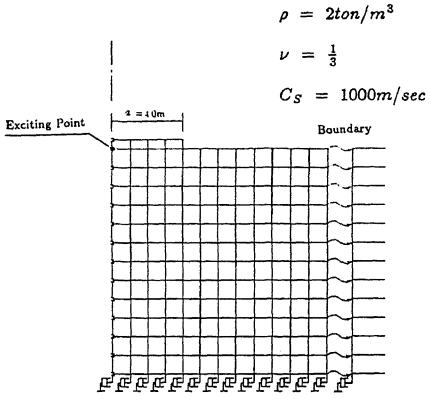

Fig. 3 Model of a Rigid Foundation on an Elastic Half Space

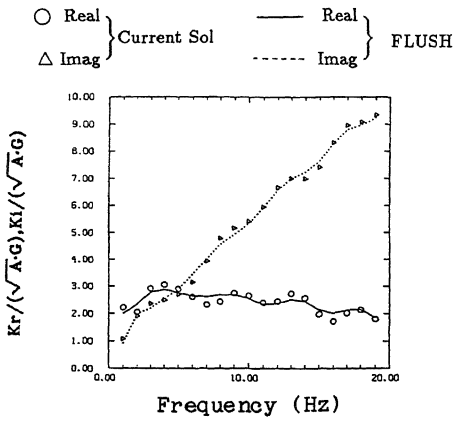

Fig. 4 Horizontal Impedance Function of a Rigid Foundation

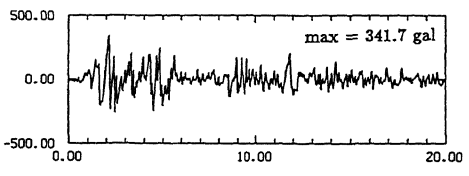

Fig. 5 Input Time History (El Centro)

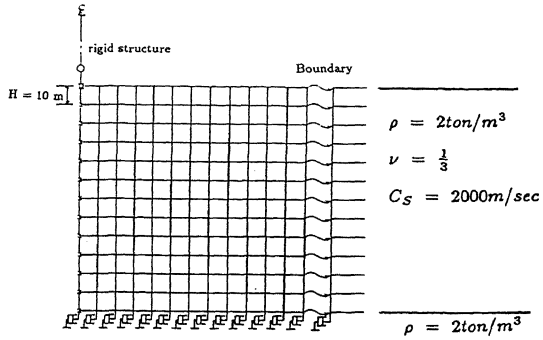

Fig. 6 A Model for Response Analysis (Case 1)

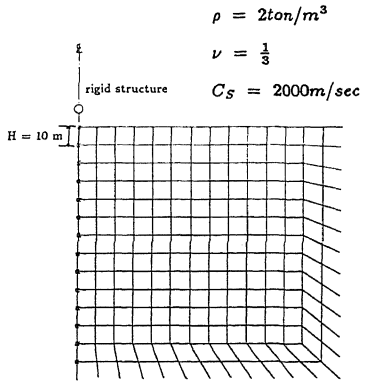

Fig. 7 A Model for Response Analysis (Case 2)

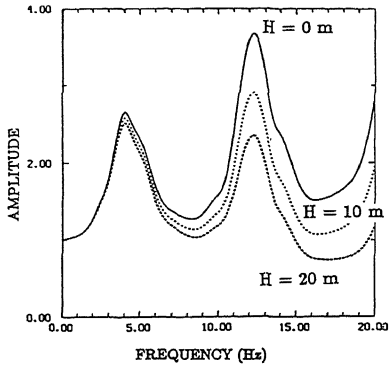

Fig. 8 Transfer Function of a Rigid Structure (Case 1)

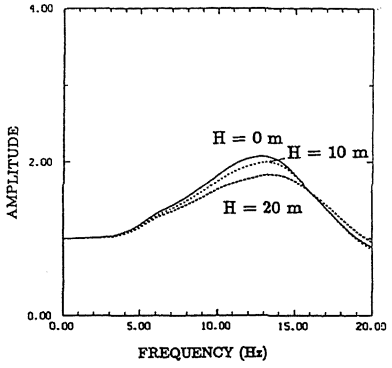

Fig. 10 Transfer Function of a Rigid Structure (Case 2)

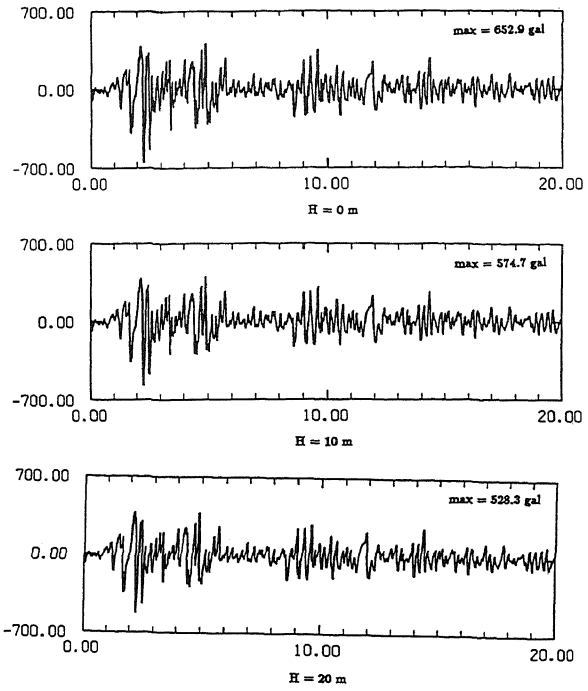

Fig. 9 Response of a Rigid Structure (Case 1)

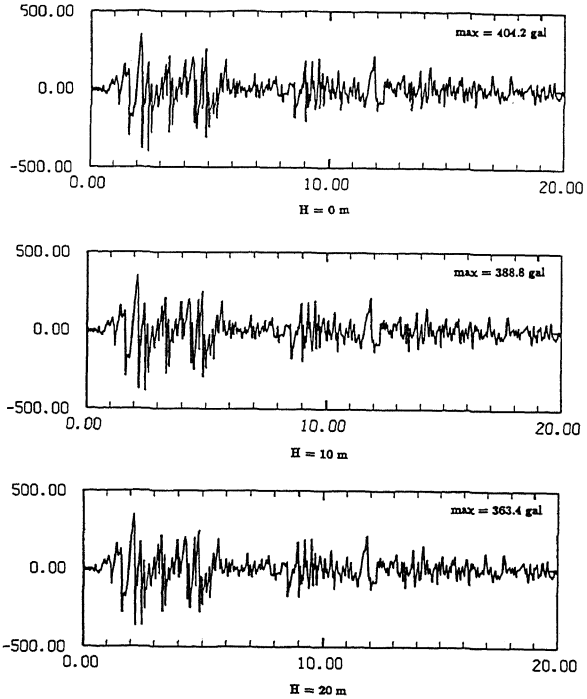

Fig. 11 Response of a Rigid Structure (Case 2)

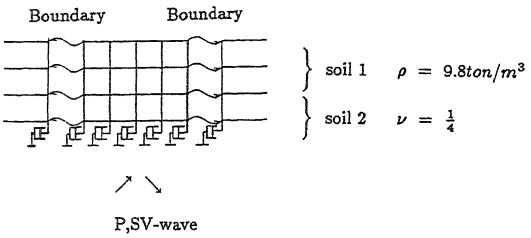

Fig. 12 The Soil Model

Table 1 Impedance Ratio

α	C_{S1}	C_{S2}
$\frac{1}{2}$	400	800
1	400	800
2	800	400

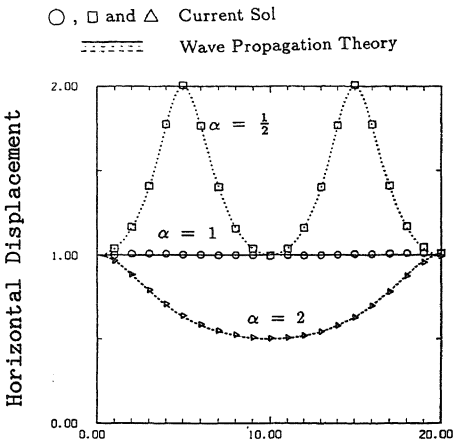

Fig. 13 Horizontal Surface Displacement due to SV-Wave

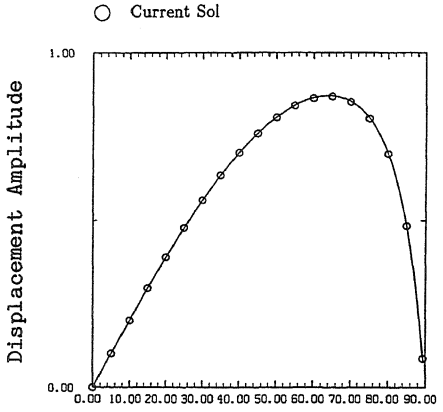

Fig. 14 Horizontal Displacement due to P-Wave

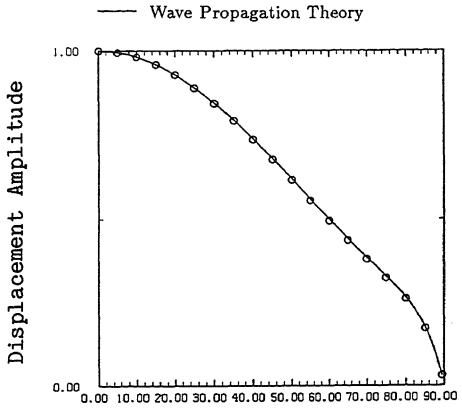

Fig. 15 Vertical Displacement due to P-Wave

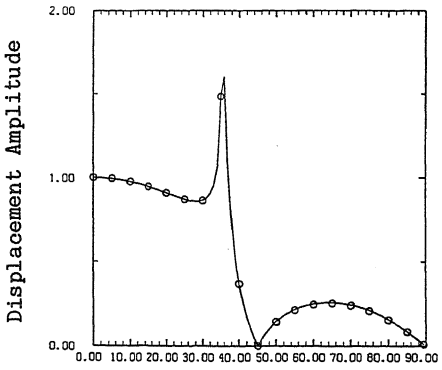

Fig. 16 Horizontal Displacement due to SV-Wave

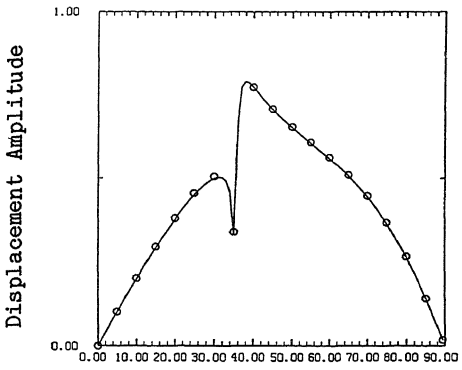

Fig. 17 Vertical Displacement due to SV-Wave